CrossMark

ORIGINAL PAPER

Local and remote climatic impacts due to land use degradation in the Amazon "Arc of Deforestation"

Maria Elisa Siqueira Silva[1] · **Gabriel Pereira**[2] · **Rosmeri Porfírio da Rocha**[3]

Abstract Many numerical studies, among them, global and regional models, have been used to simulate climatic impact due to Amazon deforestation. Most of them did not consider deforestation as usually observed and the induced dynamic changes. The present study explores the physical impacts due to Amazon deforestation by considering local and remote changes in the circulation and thermodynamics. For this, numerical experiments were conducted with RegCM3 using a relatively fine horizontal grid spacing (50 km), more realistic deforested areas (similar to the highway-network-shaped), and an updated land use map. The studied period was 2001–2006 October–March. As in most previous studies focusing on Amazon deforestation, the RegCM3-simulated air temperature increases over degraded areas, ranging from 1.0 to 2.5 °C, and precipitation decreases of around 10 %. This result is mainly related to depletion in evapotranspiration rates provided by lesser soil water extraction by the degraded vegetation. The weakening of upward motion in the mid-upper troposphere is an associated mechanism that explains the precipitation decrease after Amazon deforestation. A new result is the simulated precipitation increase, about 10 %, over the eastern South America and the adjacent South Atlantic Ocean. In these areas, the precipitation increase during October–March is associated with intensification of upper-level high pressure (the Bolivian high) coupled with negative geopotential height anomalies southeastward of the center of the high.

1 Introduction

The Amazon forest hosts more than 60 % of the world's tropical forest biodiversity and, roughly, nearly 25 % of the global biodiversity (Dirzo and Raven 2003). It is responsible for 15 % of the global terrestrial photosynthesis (Field et al. 1998). Besides its biogeophysical importance, the Amazon region is considered a global climate regulator (Betts et al. 2004). The huge air convergence at low levels, following strong surface warming, mainly during austral summer (December–January–February) periods, contributes to heat and moisture availability to be transported to distant areas, in both the Northern and Southern Hemispheres. Climate impact over the Northern Hemisphere due to tropical deforestation is mentioned, for example, by Snyder (2010), showing that anomalous adiabatic warming over Eurasia is established in response to the intensification and northward shifting of the Ferrel cell. Other studies indicate different results about how Amazon deforestation may impact the North Hemisphere. For example, Gedney and Valdes (2000) and Werth and Avissar (2002) have found some climatic impact over extratropical global areas due to Amazon deforestation, but Findell et al. (2006) found weak signals in the extratropics, even using a fine resolution numerical model. More recently, Medvigy et al. (2013) using the Ocean-Land-Atmosphere Model (OLAM; Walko and Avissar 2008) global model with finer grid spacing (25–50 km) obtained a statistically significant decrease of rainfall over the northwestern USA due to

✉ Maria Elisa Siqueira Silva
mariaelisa.siqueirasilva@gmail.com

1 Departamento de Geografia, Universidade de São Paulo, Av Prof Lineu Prestes, 338, Cidade Universitária, São Paulo, SP 05508-090, Brazil

2 Departamento de Geociências, Universidade Federal de São João del-Rei, Campus Tancredo neves, Av Visconde do Rio Preto, São João del-Rei, MG 36301-360, Brazil

3 Departamento de Ciências Atmosféricas, Universidade de São Paulo, Rua do Matão 1226, Cidade Universitária, São Paulo, SP 05508-090, Brazil

Amazon deforestation. These results indicate the need for better understanding the association between globally climatic impact and the spatial resolution used in numerical models. In South America (SA), the south-southeastward advection of water vapor and heat provided by the dominant circulation at low levels contributes to the strengthening of the South Atlantic Convergence Zone (SACZ; Marengo et al. 2004). The SACZ is an important atmospheric system contributing to the total precipitation during the summer season over a large part of SA (Carvalho et al. 2002). The advection of heat and moisture from northern SA by the South American low-level jet (SALLJ) and by the South Atlantic subtropical high circulation is also an important mechanism contributing to moisture enhancement over south-southeastern SA (Marengo et al. 2004).

Although the recognized importance of the Amazonian rainforest both in relation to climate regulation and to the hosting of a large portion of global biodiversity, the region has undergone strong deforestation since the last half century (Kirby et al. 2006). The "Arc of Deforestation", as it is called, is the main area where deforestation takes place. This area is constituted by the southern and eastern edges of the Amazonian forest and reflects the agriculture and logging expansion from the south and east of Brazil (Fearnside 2005). The Arc of Deforestation is known for its high vulnerability both due to human pressure and to its characteristic vegetation, cerrado, a savanna-like vegetation.

Many studies using atmospheric numerical modeling have been carried out in order to verify the climatic impact over SA due to land use change. All of them have considered the same paradigm: rainforest deforestation can lead to changes in climatic patterns. Deforestation of huge areas over Amazonia has shown, in general, precipitation decreasing and air temperature increasing in the global modeling studies (e.g., Malhi et al. 2008; Zhang et al. 2008; Sampaio et al. 2007; Nobre et al. 1991; Yanagi 2006; Voldoire and Royer, 2004; Berbet and Costa, 2003; Costa and Foley 2000; Manzi and Planton 1996; Henderson-Sellers et al. 1993; Lean and Rowntree 1993; Dickinson and Henderson-Sellers 1988). The spatial grid used in these general circulation model (GCM) experiments is relatively coarse, ranging from about 100 to 200 km.

Since the 1970s, numerical experiments about climatic impact due to tropical deforestation had included various types of approaches. The first studies, such as that carried out by Charney et al. (1977) focused on the use of surface albedo changes to simulate land use degradation. In this case, albedo changes were considered over great parts of Africa, Asia, and North America, with the increased albedo leading to a decrease of precipitation. Among more simplified models, Varejão-Silva et al. (1998) and Silva et al. (2006) used a meridional model to identify climatic impact following the surface degradation over the global tropical belt. They obtained

precipitation decreases and temperature enhancement as a consequence of replacement of tropical forest by short grass.

The evolution of computer power over the last four decades has allowed the use of finer resolution in numerical models, which has improved simulation results. Regional modeling over limited domains has allowed the use of finer resolutions and was applied beginning in the 1990s. Ramos da Silva et al. (2008) and Walker et al. (2009) carried out experiments with Regional Atmospheric Modeling System (RAMS) (Pielke et al. 1992), focusing on Amazon deforestation. Both studies considered a horizontal resolution of 20 km, in a restricted domain focusing on the Amazon region, and showed a precipitation decrease over deforested areas and a precipitation increase over the surroundings. While regional modeling allows the use of higher spatial resolution, the GCM's advantage is that it is not subject to forcing by lateral boundaries. To address the problem of coarse resolution in a GCM, Medvigy et al. (2011) used the OLAM GCM, a variable-resolution approach, with finer resolution (25 km) over SA and adjacent oceans. The 10-year climate simulation with OLAM under Amazon deforestation showed a decrease in precipitation over northern SA, over deforested areas, but an increase over the continental east-southeast side of SA (Medvigy et al. 2011). Otherwise, even using relatively coarse resolution (50 km) to run the regional COSMO-model (Consortium for Small-scale Modeling) for 22 years, Davin et al. (2011) obtained a precipitation decrease and temperature increase mainly over deforested Amazonian areas. The authors even noted a small precipitation increase in tropical latitudes eastward of the deforested area. In an attempt to simulate more realistic scenarios, under conditions of smaller areas with deforestation in Amazonia, simulations with mesoscale models have shown precipitation increasing over deforested areas as a result of the development of local breeze circulations forced by unequal surface heating (e.g., Khanna and Medvigy 2014; Costa et al. 2007; Roy and Avissar 2002).

From a perspective of global climatic change with concomitant land use degradation over Amazonia, some studies have shown the same signal (precipitation decrease and warming) as those from experiments carried out for past and present periods. Sampaio et al. (2007), by replacing the Amazonian rainforest by soybean and grass for six distinct future scenarios of increasing deforestation in a GCM, found warming and decreasing precipitation, mainly over the eastern Amazon region. The intensity of warming and drying in each experiment was directly related to the area deforested. In another study, considering two extrapolated scenarios of deforestation over the Amazon region to the years 2030 and 2050, Ramos et al. (2008) obtained with RAMS a decrease of precipitation for deforested areas during wet months, with greater intensity for an El Niño period compared to a La Niña period. In an experiment carried out for a larger spatial domain covering SA (from 35° S to 10° N), Canziani and Benitez (2012) considered a climate change perspective and used the PRECIS

regional model driven by ERA-40 and an ECHAM4 dataset. Considering two different deforestation scenarios, they also obtained a decrease (increase) of precipitation (temperature) over Amazonia, mainly on the eastern side of the basin; the greater climatic impact was obtained, in this case, for the scenario of larger deforestation. Over southeast SA and the Chaco Basin, sensitivity experiments showed some sign of increased precipitation.

Most numerical investigations about Amazon deforestation had been carried out with the lack of reality in extrapolating areas of degraded vegetation. In addition, it is known the great influence the Amazon region has on South America climate and its variability. In this context, the present study intends to explore the dynamical impacts due to Amazon deforestation by considering local and remote changes in the circulation and thermodynamic variables. This task is addressed using the regional model RegCM3 and a more realistic deforestation scenario for Amazonia as compiled by Soares-Filho et al. (2006).

2 Data and methods

This section describes the main model features, the design of the simulations, and the dataset used in the model validation.

2.1 Model description

The RegCM3 solves the equations for a compressible atmosphere on a finite-difference grid; it is a hydrostatic model and uses sigma-pressure vertical coordinates (Giorgi et al. 1993). The model includes a split-explicit scheme used for the time integration and a horizontal diffusion for strong topographic gradients. Heat, vapor, and momentum fluxes are calculated as functions of a drag coefficient based on similarity theory applied to the surface layer. For the atmospheric radiative transfer, the RegCM3 uses the same scheme as the Community Climate Model 3 (CCM3; Kiehl et al. 1996), where the heating rates and surface fluxes are computed in distinct ways for solar and terrestrial radiation and for clear and cloudy sky. The RegCM3 considers two schemes to treat moist processes in the atmosphere: one for deep cumulus convection (subgrid scale) and another for the precipitation resolved at grid scale. Of the available cumulus schemes in RegCM3, this study used the Grell scheme (Grell 1993), with the closure of Fritsch-Chappell, and the SUBEX scheme for grid scale precipitation as described by Pal et al. (2007). The RegCM3 has an exponential relaxation scheme at the lateral boundaries, since this permits a smoother transition between the model simulation and boundary fields (Giorgi et al. 1993).

2.2 BATS: description and modifications

The surface scheme coupled to RegCM3 isBiosphere-Atmosphere Transfer Scheme (BATS; Dickinson et al. 1993), which provides the interaction between soil surface and atmosphere through turbulent energy exchanges of water vapor, heat, and momentum. BATS presents three soil layers with the soil moisture content in each layer—upper soil, root zone, and total soil—cumulative from the surface down, each amount including that from the previous layer. The soil layers depend on vegetation type. For tropical rainforest, we defined the three layers with depths of 0.1, 3.0, and 4.5 m, while the default depths commonly used in BATS are, respectively, 0.1, 1.5, and 3.0 m. The depths of root zone and total soil layers were increased following the suggestion made by Zhang et al. (2008) and da Rocha et al. (2012). This last work showed that for the rainforest land cover, the change in soil and vegetation parameters (soil layer depth, ratio of root distribution, and hydraulic conductivity) contributes to evaporation and precipitation enhancement, which decreases the dry bias of RegCM3 over the Amazon region.

2.3 Simulation setup

Precipitation in tropical and subtropical area of SA occurs mainly during austral summer and has a significant impact on the surface processes. Although RegCM3 simulations were carried out for the whole period 1 January, 1999, through 31 March, 2007, only results from October to March, which is the rainy season for most areas of Amazon and subtropical SA (Reboita et al. 2010), are shown here. The first 2 years of simulation (1999–2000) were not included in the analysis so as to serve as a period for the model spin-up. The period 2001–2006 was specifically chosen due to the availability of observations acquired for a cerrado site located in the southeast of Brazil (northeast Sao Paulo state) and for relevance to a discussion about the ability of RegCM3 in simulating interannual variability.

The horizontal and vertical grids used for all simulations were, respectively, 50 km and 18 sigma-pressure levels. The domain, centered at (55° W, 22° S), covers the SA region with 160 longitudinal and 120 latitudinal grid points, including the area delimited by (90° W, 45° S) and (20° W, 5° N). The standard land use file in the BATS scheme, for 1993, was updated with 2005 information. To change the BATS default land use map, we altered the Network Common Data Form (NetCDF) used in the Terrain Module denominated "GLCC10MIN_BATS.CDF." The NetCDF data is divided into 21 layers, the main layer representing the land use and land cover (LULC) classes used by BATS and the other 20 layers representing the proportion of each LULC class in the pixel. In the present work, the 2005 LULC map derived from the MCD12Q1 MODIS product (for South America) and

MCD12C1 MODIS product (for other areas) was used to estimate the LULC map in BATS. Due to the inconsistency between the classification schemes used by BATS and the MCD12 product, the 17 International Geosphere-Biosphere Program (IGBP) classes were related to equivalent classes of the GLCC product. We used the Interactive Data Language (IDL) program to update the file "GLCC10MIN_BATS.CDF" with new land use data.

Results are presented for two different simulations: the control (CTRL) and the sensitivity (DEFOR). The first of these was run with the land use compiled in the Global Land Cover Characterization (http://edc2.usgs.gov/glcc) for the year 2005, GLCC 2005, shown in Fig. 1a. This CTRL simulation was used to assess the verification by contrasting it to theClimate Research Unit (CRU; Brohan et al. 2006) dataset and locally observed data. The DEFOR sensitivity experiment used a scenario of deforestation mainly on the southern-eastern borders of the Amazonian rainforest. We modified the deforestation scenario proposed by Soares-Filho et al. (2006) for the year 2050, by enhancing the current deforestation routes over the eastern and southern borders of the Amazonian forest, as shown in Fig. 1. The deforested scenario is based on GLCC 2005 land use changes by replacing rainforest and cerrado vegetation by short grass, as depicted in Figs. 1b, c. The deforestation enhancement considered in this experiment represents 14 % of the total area covered by 2005 rainforest (a minimal area was covered by cerrado vegetation). In DEFOR experiment, vegetation roughness was decreased by 96 %, and shortwave and longwave albedo were, respectively, increased by 100 and 50 % compared to the values for rainforest (Table 1). The two experiments are defined in Table 2. The climatic impacts due to the deforestation scenario are analyzed by comparing DEFOR against the CTRL run. The statistical significance of the differences between these experiments was evaluated using Student t test at 5 % significance level (Wilks, 2006).

2.4 Data

Initial and boundary conditions for the RegCM3 were provided by the NCEP/NCAR reanalysis I project (Kalnay et al. 1996) which is available at 2.5-horizontal grid, while sea surface temperatures are those compiled by NOAA/OAR/ESRL PSD, described by Reynolds et al. (2002). To describe topography and land use, the files on a 10-min horizontal grid compiled by Loveland et al. (2000) were used.

For the RegCM3 validation, monthly data from CRU were used in addition to local observations from the micrometeorological tower located over southeastern Brazil (northeast of São Paulo state) (Fig. 1c). This tower is placed in an area of environmental preservation named *Gleba Pé de Gigante* (*Pé de Gigante*, in English, Giant's Foot) reserve covered mainly by cerrado vegetation (the name refers to its shape as viewed

from space). The simulated atmospheric variables (precipitation and mean, minimum, and maximum air temperature) were compared both to CRU and local data, at daily, monthly, and seasonal scales. Local air temperature was observed at an altitude of 10 m, on the micrometeorological tower.

3 Results and discussion

Results are presented in two separate sections. In section 2.1, we provide the validation of rainy season (October–March) climatology and interannual variability of CTRL simulation against CRU and local data. In section 2.2, the climatic impact due to Amazon deforestation in the sensitivity experiment DEFOR is compared with the CTRL experiment.

3.1 Climatology and internannual variability

In general, according to Figs. 2, 3, and 4, mean air temperature and precipitation simulated by the CTRL experiment produce values close to those observed (CRU and local data) throughout the whole period analyzed. The lower air temperatures for high topography areas (in the Mantiqueira and Serra Geral mountain ranges, in southeastern and southern Brazil) simulated by CTRL are similar to CRU data (Figs. 2 and 3). Both CTRL and CRU data present milder mean values of air temperature over the southern and eastern regions of Brazil, which is physically associated with more frequent incursion of cold air masses, with higher topography elevation near the eastern coast and with the influence of the adjacent South Atlantic Ocean.

Although the spatial patterns of simulated mean air temperature are similar to that of CRU data, it is in general underestimated throughout most of the domain (Fig. 2c). The biases are mostly negative and range between 1 and 5 °C. The large negative biases of maximum air temperature over a large part of SA (Fig. 3f) help to explain the underestimation in mean values of air temperature. In most of Brazil, simulated maximum air temperature is 3 to 4 °C colder than CRU data. North of Paraguay and south of Bolivia, comprising the central region of SA, present the greatest cold biases for maximum air temperature, which are of around 5–6 °C compared with CRU data. Most of northeastern SA presents small differences between simulated and CRU maximum air temperature. The western part of Argentina over a large range of latitudes also presents negative biases for maximum air temperature, while over the western coastal belt of SA the biases are positive. In Figs. 3a, c, e, minimum air temperature simulated by CTRL depicts, in general, small and positive biases compared to CRU data. Over Brazil, the biases for minimum air temperature are small, while for the western and southwestern portions of SA, they are larger, between 1 and 5 °C. Over southern regions of SA, the positive biases in
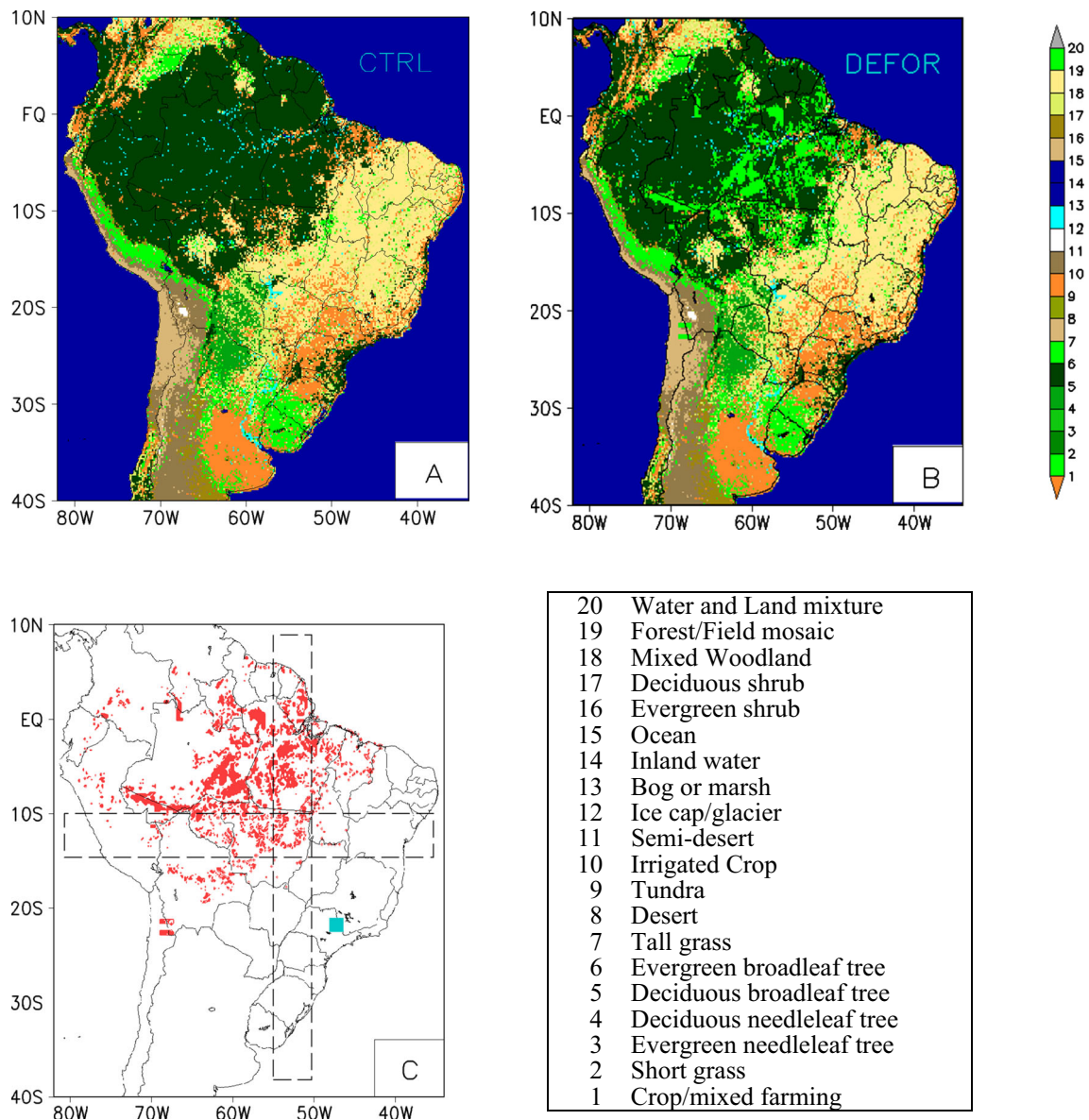
20	Water and Land mixture
19	Forest/Field mosaic
18	Mixed Woodland
17	Deciduous shrub
16	Evergreen shrub
15	Ocean
14	Inland water
13	Bog or marsh
12	Ice cap/glacier
11	Semi-desert
10	Irrigated Crop
9	Tundra
8	Desert
7	Tall grass
6	Evergreen broadleaf tree
5	Deciduous broadleaf tree
4	Deciduous needleleaf tree
3	Evergreen needleleaf tree
2	Short grass
1	Crop/mixed farming

Fig. 1 Land use maps based on GLCC classification for **a** the year 2005, for **b** deforested Amazon as extrapolated by Soares-Filho et al. (2006), and for **c** grid point vegetation class replaced by short grass instead of rainforest and cerrado. The *dashed rectangles* represent the vertical cross section areas over SA shown in Fig. 7. The *filled blue square* indicates the micrometeorological tower location. Vegetation classes are assumed to be those adopted in BATS

minimum air temperature may indicate the model's difficulty in detecting cold air mass incursions from the south.

Table 1 Physical characteristics (roughness, albedo, root zone depth, total soil layer depth) of rainforest and short grass vegetation as adopted in the CTRL and DEFOR experiments

Parameter	CTRL rainforest	DEFOR short grass	%Dif
Veg. roughness (m)	2.00	0.08	−96
Albedo OC (<0.7 μm)	0.03	0.06	+100
Albedo OL (>0.7 μm)	0.20	0.30	+50
Root zone depth (mm)	3000	1000	−67
Total soil layer (mm)	4500	3000	−33

October–March mean precipitation over SA simulated by CTRL shows spatial patterns similar to the CRU data (Figs. 2b, d). The heavier precipitation in the CRU field is climatologically associated with maximum values over the north, central, and southeast sectors of Brazil, resulting from

Table 2 Characteristics of CTRL and DEFOR experiments

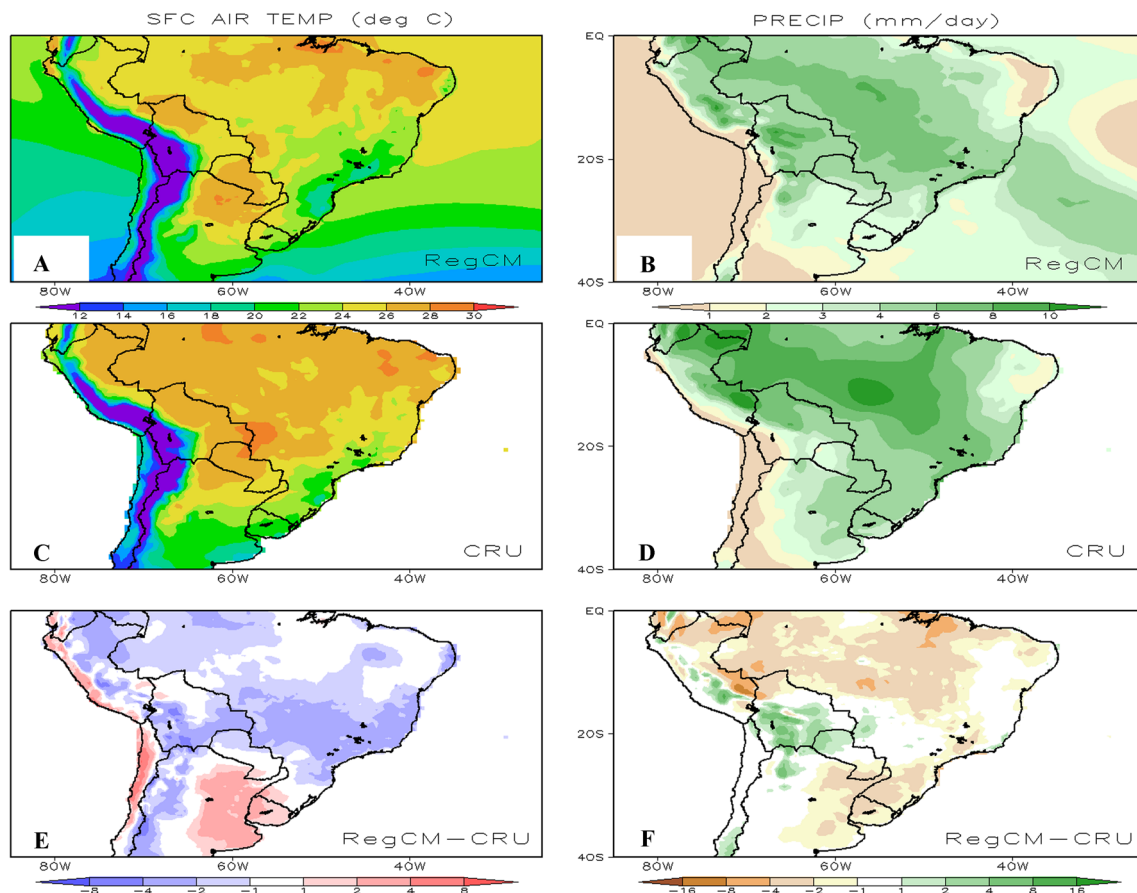| Experiment	Land use—deforestation
CTRL	GLCC 2005 (Fig. 1a)
DEFOR	GLCC 2005 + extrapolated deforestation by Soares-Filho et al. (2006) (Figs. 1b, c)

Fig. 2 **a**, **b** Mean surface air temperature (°C) and precipitation (mm day^{-1}) for the rainy season from 2001 to 2006 as simulated by RegCM3; **c**, **d** same as **a**, **b**, but for CRU observed data; **e**, **f** air temperature and precipitation differences between simulated and observed data

large convective activity due to heat availability in summer, to the monsoon-like circulation strengthening during the period, and to the coupling with the SACZ. Northeastern Brazil, the westernmost section of SA (Andean and coastal regions), and central-south Argentina are, on the other hand, characterized by low precipitation rates, as well pointed out by CRU and simulation (Figs. 2b, d). During October–March, the simulated precipitation is underestimated by CTRL, mainly over the northern (tropical) portion of Brazil (Fig. 2f). The negative biases lay between 1 and 6 mm day^{-1} (30–180 mm month^{-1}) and cover a large area of Brazil; the largest underestimation, from 4 to 8 mm day^{-1} (60–240 mm month^{-1}), occurs over the rainiest area, in a band aligned northwest-southeastern over SA. The rainfall underestimation over Amazonia region in the RegCM3 was attributed by da Rocha et al. (2012) to the small amount of water in the soil root zone with consequent reduced evapotranspiration along the year. In addition, the increase of evapotranspiration implies in a more realistic partition between sensible and latent heat fluxes as measured by the Bowen ratio.

To complement the validation of the CTRL experiment, Fig. 4a presents the time series of air temperature (minimum and maximum) daily values, just for rainy seasons, for a grid point over the cerrado station, located in southeast Brazil (indicated in Fig. 1c). Although there are systematic biases (underestimation of maximum and minimum temperatures for this site), CTRL simulates the high-frequency temporal variability in agreement with observation (Fig. 4a). While minimum air temperature presents a mean negative bias of −2.4 °C, maximum air temperature shows a mean negative bias of −3.1 °C. The negative bias for minimum temperature at the local site is not detected by comparing CTRL and CRU data (Fig. 3e). Figure 4 also presents extremes of observed minimum temperature much smaller than those simulated, with values reaching less than +10 °C, which are likely related to cold front incursions over the region. Although the simulated minimum temperature follows observed values, it never reaches the colder observed values. As for the whole SA domain, this localized comparison between CTRL and observation indicates smaller bias for minimum than maximum air temperature. The negative bias in air temperature over SA was also found by da Rocha et al. (2009) and Reboita et al. (2014) and by Giorgi et al. (2004) over Europe. These authors argue that the nonlocal boundary
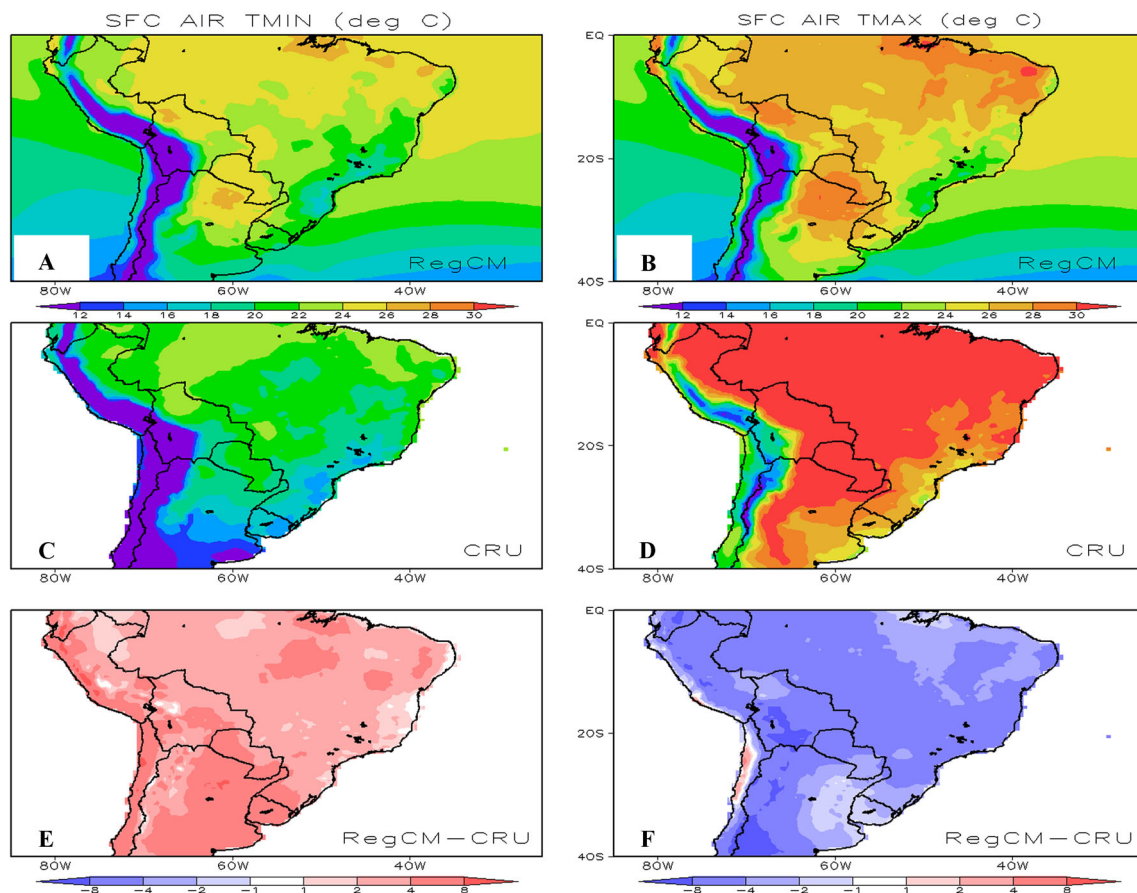
Fig. 3 **a**, **b** Minimum and maximum air temperature (°C) for the rainy season from 2001 to 2006 as simulated by RegCM3; **c**, **d** same as **a**, **b**, but for CRU observed data; **e**, **f** minimum and maximum air temperature differences between simulated and observed data

layer parameterization used in RegCM3 simulates strong vertical heat and moisture transports, leading to a relatively cooler and drier boundary layer.

Still based on cerrado site observations, Fig. 4b presents the interannual variability of the October–March mean precipitation. The precipitation amount observed at the cerrado site decreases from 2001 to 2005 but begins to increase in 2006, with the lowest value being observed in 2005. The observed and simulated interannual variability need to be interpreted with caution because they refer to only one small area of the whole domain.

3.2 Increasing deforestation over Amazon region

In this section, we present the climatic impact of deforestation over the eastern and southern areas of Amazon edges. Tropical rainforest and cerrado vegetation were replaced by short grass following the Soares-Filho et al. (2006) land use extrapolation for the year 2050, as shown in Fig. 1b, c. Time evolution of total soil water simulated over the Amazon region (60° W,15° S; 50° W, 5° S) shows that after 2 years, this variable remains stable, as also indicated in da Rocha et al. (2012). Thus, the

next figures present the averages over the rainy seasons (Oct–Mar) between 2001 and 2006.

In general, the simulated climatic impacts due to deforestation, mainly in the eastern and southern Amazon regions (indicated by the difference between DEFOR and CTRL experiments), show an air temperature increase and precipitation decrease over deforested areas (Figs. 5a, b, c). Values of variables associated with temperature (mean, minimum, and maximum and 2-m air temperature, sensible heat, and longwave fluxes) increase while specific humidity (figure not shown) and evapotranspiration rate (Fig. 5d) decrease after deforestation, mainly over the deforested areas.

While upward motion over deforested areas intensifies near the surface, at the 10-m level (Fig. 5e), in association with the temperature increase at low levels (Fig. 5c), it weakens in the middle troposphere (Fig. 5f), probably due to the decrease of convection and associated latent heating in the atmosphere. This last feature is indicated ahead in Fig. 6h. Over the eastern side of Brazil and the adjacent South Atlantic Ocean, upward motion in the mid-troposphere is intensified (Fig. 5f).

The impact on the mean precipitation (both negative and positive) shown in Fig. 5b occurred equally for all rainy seasons considered, from 2001 to 2006, and ranged from 0.1 to

Fig. 4 Time series of **a** observed and simulated maximum (*green* and *orange* colors, respectively) and minimum (*blue* and *magenta* colors, respectively) daily air temperature for the rainy seasons (Oct–Mar) from 2000–2001 to 2006–2007. The *vertical dashed lines* mark the end of each rainy season; (**b**) observed (*black*) and simulated (*red*) October–March mean precipitation (mm). The observed data are from the micrometeorological tower indicated in Fig. 1c
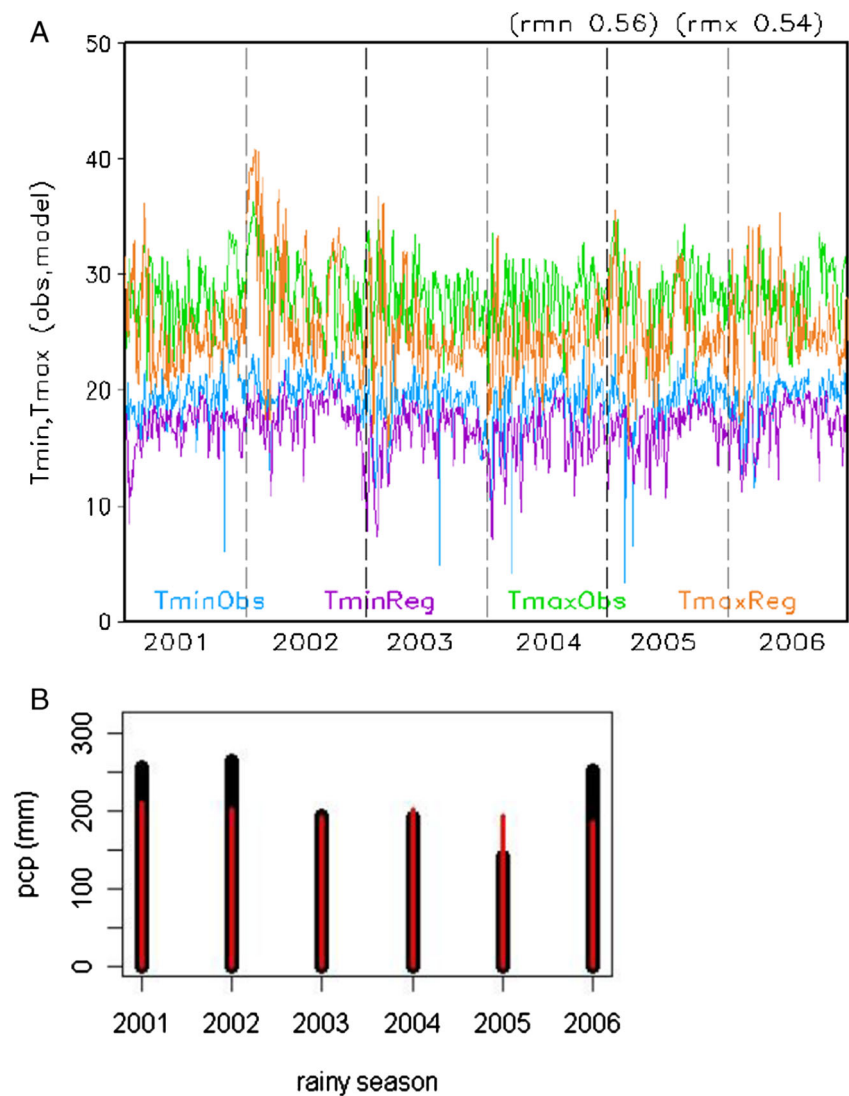
2.5 mm day^{-1} (1–75 mm month^{-1}). The precipitation decrease is mainly restricted to the deforested areas. Otherwise, over the eastern part of SA and over the adjacent South Atlantic, the deforestation over the Amazon region results in increases in mean precipitation ranging from 0.2 to 2.5 mm day^{-1}. The precipitation changes in both regions (northwestern and southeastern SA) are of the same order, about 3–20 % of climatic values. Over northeastern Brazil (~15° S–42° W), the precipitation enhancement can reach 30–40 %, since climatological values are smaller. Medvigy et al. (2011) also simulated precipitation enhancement over the eastern side of SA and its decrease over northern areas after Amazonian deforestation, which is in accordance with what is obtained in the present study. On the other hand, Lejeune et al. (2014), using the regional model COSMOS with horizontal grid spacing of 50 km, simulated mainly a precipitation decrease over northern SA and a small increase over the eastern side of Amazon as a result of Amazon deforestation. These aspects are mostly related to the decrease of evapotranspiration as vegetation is

degraded and to the consequent increase in sensible heat flux and temperature. Monthly variation in total soil moisture over the deforested region shows increased and decreased values, respectively, during the rainy and dry seasons, i.e., higher amplitude of the annual cycle is simulated by DEFOR compared to the CTRL simulation (Fig. 5g). This result may be related to lesser extraction of soil water during rainy seasons by degraded vegetation.

Large positive changes in precipitation (~2.5 mm day^{-1} or ~10 %) are also simulated over the westernmost areas of SA (northern Bolivia and southern Peru), which must be related to the increase of mass convergence due to proximity to the Andes. Similar results were obtained in the simulations of Medvigy et al. (2013). The temperature increases and the precipitation decreases over the deforested areas of northern SA are well known from past studies using coarse spatial grids in GCM simulations, as mentioned in the section 0.

The physical reason for the precipitation increase over southeastern Brazil may be revealed by other variables. An increase
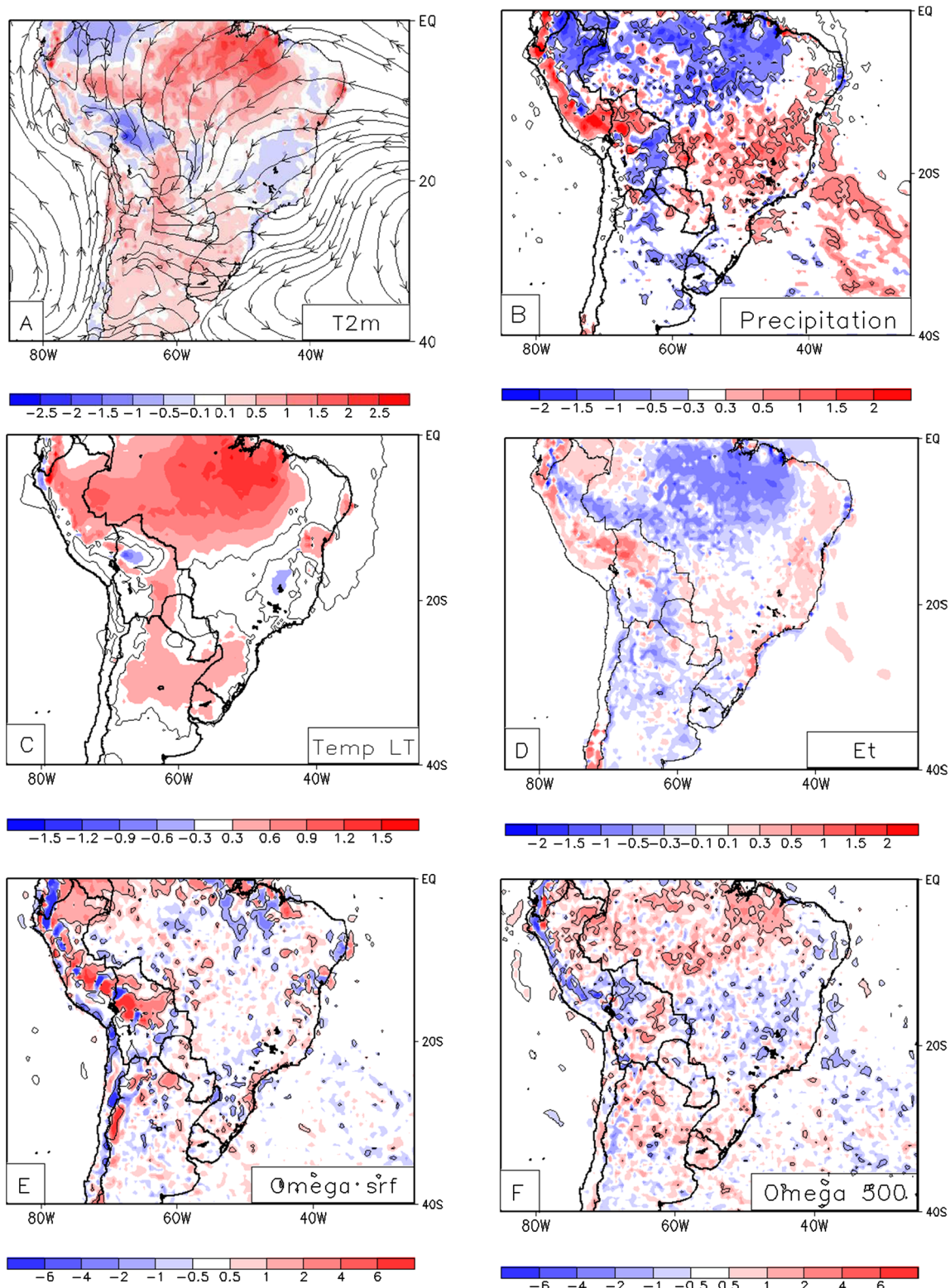
Fig. 5 Mean differences of DEFOR and CTRL experiments (DEFOR minus CTRL) for the 2001–2006 rainy seasons (Oct–Mar) for the variables: **a** air temperature (°C) at 2 m (900 hPa (circulation plotted in this frame, as reference, represents only CTRL simulation)),**b** precipitation (mm day^{-1}),**c** air temperature (°C) in lower troposphere (1000–850 hPa),**d** evapotranspiration (mm day^{-1}),**e** omega (10^{-5} hPa s^{-1}) at 10 m, and**f** omega at 500 hPa (10^{-5} hPa s^{-1}). Statistical significance at 5 % is shown by continuous *isolines* in panels **b**, **e**, and **f**
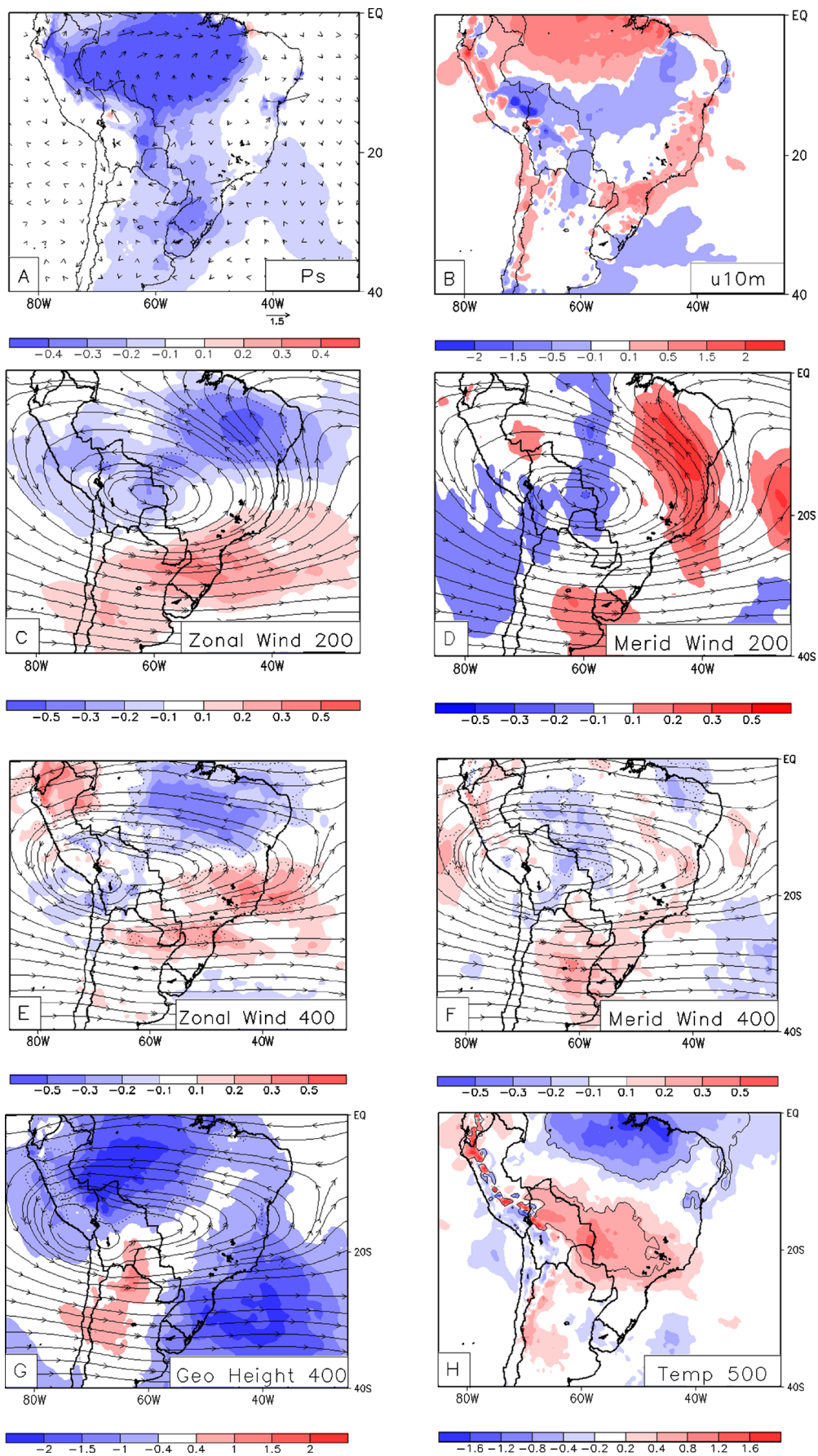
◀ **Fig. 6** Mean differences of the DEFOR and CTRL experiments (DEFOR minus CTRL) for the 2001–2006 variables: **a** surface pressure (hPa) and wind vector at 10 m (m s^{-1}), **b** zonal wind at 10 m (m s^{-1}), **c** zonal and **d** meridional winds (m s^{-1}) in the upper troposphere (200–100 hPa) (the *streamlines* plotted in frames **c** and **d** represent the 200-hPa circulation of CTRL simulation), **e** zonal and **f** meridional wind component (m s^{-1}) at 400 hP, **g** geopotential height at 400 hPa (10^{-4} mgp) (*streamlines* plotted in the frames **e**–**g** are related to the 400-hPa circulation of CTRL simulation), and h air temperature (×10 **°C**) at 700–400 hPa. Statistical significance at 5 % is shown by *black dotted isolines* in panels **c**–**g** and by *black continuous isolines* in **h** panel

of air temperature, in the lower troposphere (between 1000 and 850 hPa), was noted over the northern part of SA (Figs. 5c and 7c), reaching maximum values of 1.5–3.0 °C in the subdomain 0°–10° S and 65°–55° W (just north of SA). Over a large part of SA, a small temperature increase in the lower troposphere is still noted over Argentina, southern Brazil, Bolivia, and Paraguay (Figs. 5a, c and 7c). As surface and lower troposphere temperature rises under intensified deforestation, surface pressure decreases, mainly over the Amazon region (Fig. 6a). As thermodynamic impact of the temperature increases, there is a surface pressure lowering in large area of SA spread over western and southern Amazonia, over the central-southern SA and adjacent South Atlantic Ocean.

Following the relatively large surface pressure decrease over northern SA, it is possible to note the convergence in the warmed lower troposphere (Figs. 5a and 6a), mainly over northern SA, through the weakening of northeasterly trade winds between the Equator and 8° S. This aspect is also evident in Fig. 6b, where the changes in zonal wind component at

10 m show the weakening of the easterly wind (and northeasterly trades) from the Equator to 10° S, and its intensification between 10° S and 15–20° S. These impacts are related to the cyclonic anomalous circulation seen in Fig. 6a. The easterly weakening can be explained by the stronger warming occurring on the area delimited by 70°–45° W and 0°–8° S. Another area presenting zonal wind convergence is over the eastern and southeastern part of SA (Fig. 6b), centered close to 30° S, with weakened and intensified zonal wind to the north and south, respectively. The vertical cross section in Fig. 7c shows the air temperature increase averaged from 55° W to 50° W due to deforestation reaching the whole lower troposphere, up to 700 hPa. In the same figure, air temperature increases in the lower troposphere extending southward, reaching latitudes of 35° S. Above the layer of stronger warming (above 700 hPa), between the Equator and 10° S, deforestation implies in slight cooling due to the decrease of both convective activity and associated latent heating in the mid-upper troposphere. This effect is also evident by the difference of temperature average in the 700–400-hPa layer (Fig. 6h).

Since the climatologic circulation at low levels over SA during the rainy season is characterized by air flowing from the north-northeast to the continental south-central regions, as seen in Fig. 5a, the increase in precipitation over eastern SA would result from the moisture advection by the intensified northerly circulation (Figs. 6b and 7c). The intensified upward motion over eastern SA and the adjacent ocean (Fig. 5f) and the consequent precipitation increase can be related to the strengthening of the circulation at mid-upper troposphere (Fig. 6c–f). In these four panels of Fig. 6, the respective
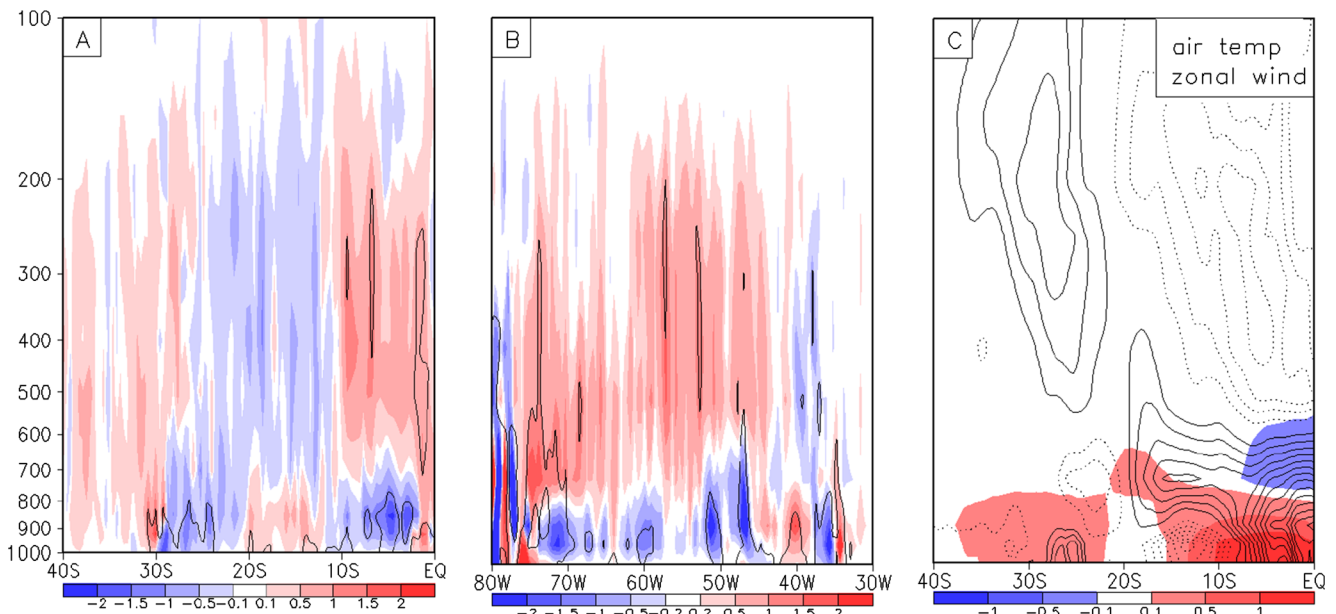

Fig. 7 Cross sections for the 2001–2006 rainy seasons of DEFOR-CTRL differences for **a** omega (10^{-5} hPa s^{-1}) in the north-south direction (averaged over 55° W–50° W); **b** omega (10^{-5} hPa s^{-1}) in the west-east direction (averaged over 15° S–10° S); **c** as in **a**, but for air temperature (shading with scale at the bottom in °C) and zonal wind (*isolines* at each 0.1 m s^{-1}). Statistical significance at 5 % is shown by *black isolines* in panels **a** and **b**

streamlines for the CTRL are overlaid on the shaded DEFOR-CTRL difference fields. At 400 hPa (Fig. 6e, f), the impact of deforestation is represented by easterly (westerly) flow intensification on the northern (southeastern) side of the longitudinally elongated high pressure (centered in ~18° S) and by northerly (southerly) flow intensification on its western (eastern) side. This configuration means the intensification, or its eastward displacement, of high pressure at middle levels after deforestation experiment. The impact on upper-level (200–100 hPa) circulation (Fig. 6c, d) is similar to that for middle levels, except that at these levels, the high pressure presents more circular shape.

In subtropical latitudes (20–40° S), the difference (DEFOR-CTRL) of geopotential height at 400 hPa shows positive and negative anomalies (Fig. 6g), respectively, centered in 65° W and 40° W. These anomalies must be related to the intensification of convective activity displaced southward and westward of the Amazon Basin (Fig. 5c). According to Lenters and Cook (1997), at upper levels, the formation of high and low pressure systems is expected, respectively, southwestward and southeastward of the region of maximum diabatic heating due to convective activity. In addition, in Fig. 6g, the southwestward positive anomaly of geopotential indicates an intensification of the Bolivian high, while the negative anomaly eastward could explain the more intense rainfall in eastern SA and adjacent South Atlantic Ocean. The southeastward intensification of convection in DEFOR experiment is highlighted by the enhancement of upward motion at mid troposphere between 12 and 30° S (Fig. 7a) and warming at mid troposphere (Fig 6h). Therefore, besides the local impact of the land use degradation, the present paper shows remote induced changes in the SA circulation with consequent changes of precipitation over a large area (Fig. 5b).

Additionally, vertical motion cross sections (Fig. 7) are analyzed in north-south and west-east directions respectively averaged for the bands 15° S–10° S and 55° W–50° W. In the north-south cross section, the mean upward motion weakens from middle to upper troposphere just above the deforested region, from the Equator to 10° S, while further south, from 10° S to 20° S, it intensifies (Fig. 7a). In the lower troposphere (up to 650–700 hPa), the opposite changes in vertical motion are noted: while the northern region (0–10° S) is characterized by stronger upward motion, the southern one (10° S–20° S) presents weaker upward motion. This aspect was already noted in other studies considering climatic impact due to deforestation (e.g., Lejeune et al. 2014), and it is physically related to a breeze-like circulation anomaly developed at the regional scale due to differential near-surface warming. The enhancement upward motion at low levels over 0–10° S region would be the result of the surface and low-level warming shown in Fig. 5a, c and Fig. 7c. In this latitudinal belt, the weakening of upward motion from mid-upper troposphere must be related to

the decrease in latent heat release, following the mean decrease in evapotranspiration and precipitation rates. The decrease and increase, respectively, of upward motion in the low and middle-to-high troposphere, further south (from 10° S to 20° S in Fig. 7a), could result from the circulation located in the region further north (Equator–10° S). Over the 28° S–40° S latitude belt, a region commonly characterized by subtropical subsidence, there is a strengthening of the downward motion (Fig. 7a).

In the west-east cross section (Fig.7b), the impact of deforestation in vertical motion at middle to upper levels is clearly identified. Eastward of 40° W, the upward motion is intensified (or downward motion is weakened), while toward the west, the upward motion is weakened (or downward motion is intensified). The enhancement of precipitation to the east is similar to the result obtained by Lejeune et al. (2014). Along this same section, the impact on vertical motion at low levels is opposite in sign to that obtained for the middle to upper troposphere. Stronger values in the westernmost regions, close to 75° W, are probably related to convergence and forced upward motion (which is also seen in Fig. 5e, f) when air flows westward and encounters the Andes mountain barrier.

Although the air temperature changes due to deforestation are mainly noted in the low troposphere, from the Equator to 35° S, the whole troposphere is affected as shown by zonal wind component cross section in Fig. 7c. While northward of 20° S there is an intensification of westward flow in the mid-upper troposphere (Fig. 7c), the southern strip presents an eastward anomaly, which characterizes the high pressure system's intensification (or its eastward displacement, which of these is not yet clear), as seen in Fig. 6c–f. As depicted in Fig. 6b, the zonal wind confluence seen at low levels, in tropical latitudes, is also clear in the Fig. 7c, close to 8° S. In addition, low-level zonal wind confluence at subtropical latitudes over eastern SA (Fig. 6b) is also seen in Fig. 7c close to 28° S, but it is weaker and shallower than the tropical one.

4 Discussion and conclusion

This study investigated the climatic impact over SA due to the increasing of deforestation in the Amazon Arc of Deforestation region. The land use impact was analyzed by replacing the Amazon rainforest and cerrado vegetations by short grass under the BATS classification. RegCM3 was run for 2001–2006 rainy seasons (October–March), which was validated by comparing with CRU and micrometeorological tower data located in southeastern Brazil.

RegCM3 simulations of spatial patterns of temperature and precipitation over South America were similar to those observed, except for some aspects highlighted. RegCM3 underestimates and overestimates maximum and minimum air temperature, respectively. Over most of Brazil, minimum

temperature bias (comparing to CRU data) is very small while maximum temperature negative bias varies over the range 3–5 °C. Over Argentina and the Andean region, minimum temperature positive bias is in the range 3–5 °C. The negative bias in simulated mean air temperature near the surface is mainly due to the underestimation in the maximum air temperature. The RegCM3 also shows precipitation underestimation over the rainiest tropical areas (the northwest-southeast band crossing SA). The negative bias in air temperature and precipitation by RegCM3 is also reported in da Rocha et al. (2009). The comparison to local observations indicates that the RegCM3 does not reproduce all aspects of observed interannual variability of the precipitation, indicating that more effort must be made in this direction.

In general, the RegCM3 simulation indicates that vegetation degradation in the Amazon region implies an air temperature increase and precipitation decrease over the degraded area, that is, over northern SA. Precipitation decrease is also simulated over southern Bolivia and northern Argentina. Over degraded areas, precipitation decreases are related to the decrease of short grass roughness and root zone soil layer depth, which provides less water to be transferred to atmosphere with consequent decrease of evapotranspiration. These results are in agreement with those obtained by many similar studies using global or regional models (Malhi et al. 2008; Sampaio et al. 2007; Yanagi 2006, Medvigy et al. 2011 and Lejeune et al. 2014). Differently from most studies in this subject, the present paper shows precipitation increasing over the eastern side of SA and adjacent South Atlantic Ocean, as also found by Medvigy et al. (2011). In comparison to results from coarser resolution GCMs, this precipitation increase may be partially related to the increase of the horizontal resolution used in the present simulation (50 km). After deforestation, the temperature increase does not remain restricted to northern SA but spreads over southern parts. Due to the increase in temperature and the surface pressure decrease, anomalous low-level convergence occurs over northern SA. This convergence results of northeasterly trade wind intensification and weakening, respectively, over northwestern and southeastern Amazon. On the other hand, western Amazon undergoes precipitation increase associated with moisture increase resulting from easterly wind intensification after Amazon deforestation.

The heavier (or more frequent) precipitation over the eastern side of SA simulated by RegCM3 in the deforestation scenario is physically related to changes in the circulation. Strengthening the upper-level Bolivian high is related to warming in the low-middle troposphere. At middle levels (400 hPa), the trough southeastward of this high pressure center is strengthened after land use degradation, providing upward motion intensification over eastern SA and oceanic adjacent areas. Thus, the precipitation enhancement in areas of eastern SA is associated with strengthening of high pressure at upper levels. The moisture advection by the intensification of

northeasterly winds at low levels, not yet investigated, must also contribute to the precipitation increase in this area following Amazon rainforest degradation.

Thus, the use of the RegCM3 regional model with medium resolution (50 km) and large domain to evaluate the climatic impact over SA due to Amazonian partial deforestation provided two main results: precipitation decreases over northern regions and precipitation increases over southeastern SA and adjacent South Atlantic regions. In accord with past studies involving climate modeling, the first result is depicted as a consequence of deforestation, while the second is rarely mentioned in the literature. Dynamical analysis carried out provided deeper comprehension of climatic impact following land use degradation that sustains the precipitation increase in eastern SA. Even so, it is not clear what differences cause the climate models to present different responses. It is still necessary to investigate the influence generated by the use of different spatial resolutions and by different surface schemes in simulations conducted by the same model.

From a climatic change point of view, many observational studies have indicated precipitation increases over many areas of SA, including its eastern side, the area delimited by Equator–20° S and 65° W–45° W (Marengo et al. 2012; Haylock et al. 2006; Liebmann et al. 2004). In the present study, increases of precipitation over eastern SA were also simulated, associated with the Amazon deforestation. In both frameworks, deforestation and climate change, the precipitation increase is of the same order, about 10 % in relation to climatological values. Thus, one question for further investigation is what is the contribution from each aspect? Is the climatic change or the Amazonian land use degradation the most important cause for the increase in precipitation over portions of eastern South America?

References

Berbet, MLC, Costa MH (2003) Climate change after tropical deforestation: seasonal variability of surface albedo and its effects on precipitation change, J Clim, 16, 2099 – 2104. doi:10.1175/1520-0442(2003)016<2099:CCATDS>2.0.CO;2

Betts RA, Cox PM, Collins M, Harris PP, Huntingford C, Jones CD (2004) The role of ecosystem-atmosphere interactions in simulated Amazonian precipitation decrease and forest dieback under global climate warming. Teor Appl Climatol 78:157–175. doi:10.1007/s00704-004-0050-y

Brohan P, Kennedy JJ, Harris I, Tett SFB, Jones PD (2006) Uncertainty estimates in regional and global observed temperature changes: a

new dataset from 1850. J Geophys Res 111:D12106. doi:10.1029/2005JD006548

Canziani PO; Benitez GC (2012) Climate impacts of deforestation/land-use changes in central South America in the PRECIS Regional Climate Model: mean precipitation and temperature response to present and future deforestation scenarios. Volume 2012, Article ID 972672, 20 pages doi:10.1100/2012/972672

Carvalho LMV, Jones C, Liebmann B (2002) Extreme precipitation events in southeastern South America and large-scale convective patterns in the South Atlantic convergence zone. J Clim 15:2377–2394.

Charney J, William JQ, Shu-hsien C, Kornfield J (1977) A comparative study of the effects of albedo change on drought in semi-arid regions. J Atmos Sci 34:1366–1385. doi:10.1175/15200469(1977)034<1366:ACSOTE>2.0.CO;2

Costa MH, Foley JA (2000) Combined effects of deforestation and doubled atmospheric CO2 concentrations on the climate of Amazonia. J Clim 13:18–34. doi:10.1029/2007GL030612

Costa MH, Yanagi SNM, Souza PJOP, Ribeiro A, Rocha EJP (2007) Climate change in Amazonia caused by soybean cropland expansion, as compared to caused by pastureland expansion. Geophys Res Lett 34:L07706. doi:10.1029/2007GL029271

da Rocha RP, Morales CA, Cuadra SV, Ambrizzi T (2009) Precipitation diurnal cycle and summer climatology assessment over South America: an evaluation of Regional Climate Model version 3 simulations. J Geophys Res 114:D10108. doi:10.1029/2008JD010212

da Rocha RP, Cuadra SV, Reboita MS, Kruger LF, Ambrizzi T, Krusche N (2012) Effects of RegCM3 parameterizations on simulated rainy season over South America. Clim Res 52:253–265. doi:10.3354/cr01065

Davin EL, Stockli R, Jaeger EB, Levis S, Seneviratne SI (2011) COSMO-CLM2: a new version of the COSMO-CLM model coupled to the community land model. Clim Dyn 37:1889–1907. doi:10.1007/s00382-011-1019-z

Dickinson RE, Henderson-Sellers A (1988) Modelling tropical deforestation: a study of GCM land-surface parameterizations. QJR Meteorol Soc 114:439–462

Dickinson RE, Henderson-Sellers A, Kennedy PJ (1993) Biosphere-atmosphere transfer scheme (BATS) version 1E as coupled to the NCAR community climate model. NCAR Tech. Note, NCAR/TN-387. National Center for Atmospheric Research, Boulder

Dirzo R, Raven PH (2003) Global state of biodiversity and loss. Annu Rev Environ Resour 28:137–167.

Fearnside P (2005) Deforestation in Brazilian Amazonia: history, rates, and consequences. Conserv Biol 19(3):680–688

Field CB, Behrenfeld MJ, Randerson JT, Falkowski P (1998) Primary production of the biosphere: integrating terrestrial and oceanic components. Science 281:237–240.

Findell KL, Knutson TR, Milly PCD (2006) Weak simulated extratropical responses to complete tropical deforestation. J Clim 19:2835–2850.

Gedney N, Valdes PJ (2000) The effect of Amazonian deforestation on the Northern Hemisphere circulation and climate. Geophys Res Lett 27:3053–3056

Giorgi F, Marinucci MR, Bates GT, DeCanio G (1993) Development of a second generation regional climate model (RegCM2). Part II: convective processes and assimilation of lateral boundary conditions. Mon Weather Rev 121: 2814−2832

Giorgi F, Bi XI, Pal JS (2004) Mean, inter-annual variability and trends in a regional climate change experiment over Europe. I. Present-day climate (1961–1990). Clim Dyn 22:733–756. doi:10.1007/s00382-004-0409-x

GLCC (2005) Global Landcover 2000, http://www.gvm.jrc.it/glc2000/ See also http://edcdaac.usgs.gov/glcc/globdoc2 0.asp

Grell G (1993) Prognostic evaluation of assumptions used by cumulus parameterizations. Mon Weather Rev 121:764–787

Haylock MR, Peterson TC, Alves LM, Ambrizzi T, Anunciação MT, Baez J, Barros VR, Berlato MA, Bidegain M, Coronel G, Corradi V, Garcia VJ, Grimm AM, Karoly D, Marengo JA, Marino MB, Moncunill DF, Nechet D, Quintana J, Rebello E, Rusticucci M, Santos JL, Trebejo I, Vicent L (2006) Trends in total and extreme South American rainfall 1960-2000 and links with sea surface temperature. J Clim 19(8):1490–1512

Henderson-Sellers A, Dickinson RE, Durbidge TB, Kennedy PJ, McGuffie K, Pitman AJ (1993) Tropical deforestation: modeling local to regional scale climate change. J Geophys Res 98:7289–7315

Kalnay E et al. (1996) The NCEP/NCAR 40-year reanalysis project. Bull Am Meteorol Soc 77:437–470.

Khanna J, Medvigy D (2014) Surface roughness variations control the regional atmospheric response to contemporary deforestation in Rondonia, Brazil. J Geophys Res - Atmos 119:13067–13078. doi:10.1002/2014JD022278

Kiehl JT, Hack JJ, Bonan GB, Boville BA, Briegleb BP, Williamson DL, Rash PJ (1996) Description of the NCAR Community Climate Model (CCM3). NCAR/TN-420 +

Kirby KR, Laurance WF, Albernaz AK, Schroth G, Fearnside PM, Scott B, Venticinque EM, Costa C (2006) The future of deforestation in the Brazilian Amazon. Futures 38(4):432–453. doi:10.1016/j.futures.2005.07.011

Lean J, Rowntree PR (1993) A GCM simulation of the impact of Amazonian deforestation on climate using an improved canopy representation. QJR Meteorol Soc 119:509–530. doi:10.1002/qj.49711951109

Lejeune Q, Davin EL, Guillod BP, Seneviratne SI (2014) Influence of Amazonian deforestation on the future evolution of regional surface fluxes, circulation, surface temperature and precipitation. Clim Dyn. doi:10.1007/s00382-014-2203-8

Lenters JD, Cook KH (1997) On the origin of the Bolivian high and related circulation features of the South American climate. J Atmos Sci 54:656–678

Liebmann B, Vera CS, Carvalho LMV, Camilloni IA, Hoerling MP, Allured D, Barros VR, Báez J, Bidegain M (2004) An observed trend in central south American precipitation. J Clim 17:4357–4367. doi:10.1175/3205.1

Loveland TR, Reed BC, Brown JF, Ohlen DO, Zhu J, Yang L, Merchant JW (2000) Development of a Global Land Cover Characteristics database and IGBP DISCover from 1-km AVHRR data. Int J Remote Sens 21(6/7):18–51. doi:10.1007/978-3-540-37294-3_3

Malhi Y, Timmons RJ, Betts RA, Killeen TK, Li W, Nobre CA (2008) Climate change: deforestation, and the fate of the Amazon. Science 319(5860):169–172. doi:10.1126/science.1146961

Manzi AO, Planton S (1996) A simulation of Amazonian deforestation using a GCM calibrated with ABRACOS and ARME data. In: Gash JHC, Nobre C, Roberts JM, Victoria RL (eds) Amazonian deforestation and climate. Wiley, Chicester, pp. 505–529

Marengo JA, Soares W, Saulo C, Nicolini M (2004) Climatology of the LLJ east of the Andes as derived from the NCEP reanalyses. J Clim 17:2261–2280

Marengo JA, Liebmann B, Grimm AM, Misra V, Silva Dias PL, Cavalcanti IFA, Carvalho LMV, Berbery EH, Ambrizzi T, Vera CS, Saulo AC, Nogues-Paegle J, Zipser E, Seth A, Alves LM (2012) Recent developments on the South American monsoon system. Int J Climatol 32:1–21. doi:10.1002/joc.2254

Medvigy D, Walko RL, Avissar R (2011) Effects of deforestation on spatiotemporal distributions of precipitation in South America. J Clim 24:2147–2163. doi:10.1175/2010JCLI3882.1

Medvigy D, Walko RL, Otte MJ, Avissar R (2013) Simulated changes in northwest US climate in response to Amazon deforestation. J Clim 26:9115–9136. doi:10.1175/JCLI-D-12-00775.1

Nobre CA, Sellers PJ, Shukla J (1991) Amazonian deforestation and regional climate change. J Clim 4:957–988

Pal JS Coauthors (2007) Regional climate modeling for the developing world: the ICTP RegCM3 and RegCNET. Bull Am Meteorol Soc 88:1395–1409

Pielke RE Coauthors (1992) A comprehensive meteorological modeling system—RAMS. Meteorog Atmos Phys 49:69–91

Ramos da Silva R, Werth D, Avissar R (2008) Regional impacts of future land-cover changes on the Amazon basin wet-season climate. J Clim 21:1153–1170. doi:10.1175/2007JCLI1304.1

Reboita MS, Gan MA, da Rocha RP, Ambrizzi T (2010) Regimes de precipitação na américa do Sul: uma revisão bibliográfica. Revista Brasileira de Meteorologia 25:185–204

Reboita MS, Fernandez JPR, Llopart MP, da Rocha RP, Pampuch LA, Cruz FT (2014) Assessment of RegCM4.3 over the CORDEX South America domain: sensitivity analysis for physical parameterization schemes. Clim Res 60:215–234. doi:10.3354/cr01239

Reynolds RW, Rayner NA, Smith TM, Stokes DC, Wang W (2002) An improved in situ and satellite SST analysis for climate. J Clim 15: 1609–1625

Roy BS, Avissar R (2002) Impact of land use/land cover change on regional hydrometeorology in Amazonia. J Geophys Res 107(D20). doi:10.1029/2000JD000266

Sampaio G, Nobre N, Costa MH, Satyamurty P, Soares-Filho BS, Cardoso M (2007) Regional climate change over eastern Amazonia caused by pasture and soybean cropland expansion. Geophys Res Lett vol. 34,no.17, article L17709, 2007

Silva MES, Franchito SH, Rao VB (2006) Effects of Amazonian deforestation on climate: a numerical experiment with a coupled biosphere-atmosphere model with soil hydrology. Theor Appl Climatol, Austria 85:1–18. doi:10.1007/s00704-005-0177-5

Snyder PK (2010) The influence of tropical deforestation on the Northern Hemisphere climate by atmospheric teleconnections. Earth Interact 14:1–34. doi:10.1175/2010EI 280.1

Soares-Filho BS Coauthors (2006) Modelling conservation in the Amazon basin. Nature 440:520–523. doi:10.1038/nature04389

Varejão-Silva MA, Franchito SH, Rao VB (1998) A Coupled Biosphere-Atmosphere Climate model suitable for studies in climatic change due to land surface alterations. J Clim Estados Unidos, 11, 7: 1749-1767. doi: 10.1175/1520-0442(1998)011<1749:ACBACM>2.0.CO;2

Voldoire AJ, Royer JF (2004) Tropical deforestation and climate variability. Clim Dyn 22:857–874. doi:10.1007/s00382-004-0423-z

Walker R, Moore NJ, Arima E, Perz S, Simmons C, Caldas M, Vergara D, Bohrer C (2009) Protecting the Amazon with protected areas. Proc Natl Acad Sci 106:10582–10586. doi:10.1073/pnas.0806059106

Walko RL, Avissar R (2008) The Ocean–Land–Atmosphere Model (OLAM): formulation and tests of the nonhydrostatic dynamic core. Mon Weather Rev, 136, 4045–4062

Werth D, Avissar R (2002) The local and global effects of Amazon deforestation. J Geophys Res 107:8087. doi:10.1029/2001JD000717

Wilks DS (2006) Statistical methods in the atmospheric sciences: an introduction, 2nd edn. Academic Press, San Diego, p. 627

Yanagi SNM (2006) Albedo of an Amazon tropical rainforest: field measurements, remote sensing, modeling, and its influence on the regional climate. PhD Thesis,Federal University of Viçosa, Brazil (available at www.tede.ufv.br)

Zhang Y, Fu R, Yu H, Dickinson RE, Juarez RN, Chin M, Wang H (2008) A regional climate model study of how biomass burning aerosol impacts land−atmosphere interactions over the Amazon. J Geophys Res 113: D14S15. doi: 10.1029/2007 JD 009449